Real-Time RT-PCR Assay for Quantifying Cyclin D1 mRNA in B-Cell Non-Hodgkin's Lymphomas

L. Jeffrey Medeiros, M.D., Seema Hai, B.S., Vilmos A. Thomazy, M.D., Oscar C. Estalilla, M.D., Jorge Romaguera, M.D., Rajyalakshmi Luthra, Ph.D.

From the Departments of Hematopathology (LJM, SH, VAT, OCE, RL) and Lymphoma/Myeloma (JR), The University of Texas M.D. Anderson Cancer Center, Houston, Texas

Mantle cell lymphoma (MCL) is a distinct type of non-Hodgkin's lymphoma (NHL) characterized by the t(11;14)(q13;q32), in which the *ccnd*1 gene is juxtaposed with the immunoglobulin heavy chain gene, resulting in up-regulation of cyclin D1. Cyclin D1 overexpression is a useful finding that supports the diagnosis of MCL. In this study, we used a 5' → 3' exonuclease-based real-time reverse-transcriptase polymerase chain reaction (RT-PCR) method to quantify cyclin D1 mRNA in 108 B-cell NHL and nonneoplastic specimens, including 25 cases of MCL. Glyceraldehyde-3-phosphate dehydrogenase (GAPDH) was also quantified to normalize cyclin D1 mRNA levels, and the data were expressed as a cyclin D1 to GAPDH ratio. At each anatomic site, MCL cases had higher cyclin D1 levels than other types of NHL or nonneoplastic specimens, without overlap. For example, in lymph node specimens, the median cyclin D1/GAPDH ratio was 147 (range, 94–160) in MCL, compared with 8.6 (range, 4–18) in chronic lymphocytic leukemia/small lymphocytic lymphoma; 5.8 (range, 1.8–24) in follicular lymphoma; 4.8 in one case of marginal zone lymphoma; and 20.2 (range, 5.8–44) in reactive specimens. Statistical analysis using one-way analysis of variance (ANOVA) showed that MCL cases had significantly higher cyclin D1 levels than other groups ($P < .05$). In peripheral blood specimens involved by MCL, cyclin D1 levels correlated with extent of involvement. We conclude that this real-time RT-PCR method to quantify cyclin D1 expression is helpful in distinguishing MCL from other types of B-cell NHL and from nonneoplastic specimens. This method is rapid, can be applied to the analysis of fluid specimens, and obviates the need for time-consuming and laborious detection methods that are required by traditional semi-quantitative RT-PCR methods.

KEY WORDS: Cyclin D1, Mantle cell lymphoma, Quantitative reverse-transcriptase polymerase chain-reaction, Real-time.

Mod Pathol 2002;15(5):556–564

Mantle cell lymphoma (MCL) is a clinically aggressive type of B-cell non-Hodgkin's lymphoma (NHL) that represents approximately 6% of all NHL in North America (1). A constant feature of MCL is the presence of the t(11;14)(q13;q32), in which the *ccnd*1 gene on chromosome 11q13 is juxtaposed with the joining region of the immunoglobulin heavy chain (IgH) gene on chromosome 14q32, resulting in up-regulation and overexpression of cyclin D1 (2). Cyclin D1 forms a complex with cyclin-dependent kinase 4 and interacts with other proteins to promote transition of the cell cycle from G1 to S phase (2, 3). Cyclin D1 overexpression is characteristic of MCL and is rare in other types of B-cell NHL (4, 5).

Histologically, MCL can be difficult to distinguish from other types of B-cell NHL. Nevertheless, this distinction is important because MCL patients have a poorer prognosis and require more aggressive therapy than patients with low-grade B-cell NHL. Thus, detection of the t(11;14) has become an important tool in differential diagnosis (6). However, current methods to assess for the t(11;14) have limitations. Southern blot hybridization can detect bcl-1 locus rearrangements consistent with the t(11;14) in ≤75% of MCL cases if multiple genomic probes are used (7, 8). However, this technique requires large amounts of high-quality DNA and is labor intensive. In addition, hybridization with multiple probes often requires stripping and rehybridization of membranes, a time-consuming process that prolongs turnaround time. PCR assays to detect the t(11;14) are convenient, require relatively small amounts of DNA, and can be performed using fixed, paraffin-embedded tissue. However,

VOL. 15, NO. 5, P. 556, 2002 Printed in the U.S.A.
Date of acceptance: January 28, 2002.
Address reprint requests to: L. Jeffrey Medeiros, M.D., Department of Hematopathology, Box 72, The University of Texas M.D. Anderson Cancer Center, 1515 Holcombe Boulevard, Houston, TX 77030.

currently available assays only detect translocations involving the major translocation cluster region, involved in approximately 40–50% of cases of MCL (9–12). More recently, fluorescence *in situ* hybridization methods have become popular because large probes can be used to detect the widely scattered breakpoints on chromosome 11. Using these methods, the t(11;14) can be detected in >95% of MCL cases (13–15).

Alternatively, methods for assessing cyclin D1 overexpression have been employed, because all chromosome 11 breakpoints theoretically result in cyclin D1 overexpression. Standard Northern blot analysis may be used, but these methods require fresh tissue and meticulous and time-consuming laboratory methods (16, 17). In contrast, immunohistochemical methods are far easier and very popular in pathology laboratories (4, 5). However, these methods may have limited sensitivity in cases that are not optimally fixed and processed (18, 19). Furthermore, most immunohistochemical assays are not optimized for assessing peripheral blood and bone marrow aspirate smears.

To circumvent these problems, we developed a 5' → 3' exonuclease-based quantitative real-time reverse-transcriptase polymerase chain reaction (RT-PCR) assay to assess cyclin D1 mRNA levels in MCL and other types of B-cell NHL and nonneoplastic specimens. The assay is simple, rapid, and does not require cumbersome dilution steps involved in traditional semi-quantitative RT-PCR assays. Furthermore, real-time RT-PCR methods allow collection of data points in the exponential phase of PCR, as opposed to many conventional quantitative PCR assays, which use end points, allowing for more accurate quantification of target (20–22).

MATERIALS AND METHODS

We analyzed 108 fresh or frozen specimens representing various types of B-cell NHL and nonneoplastic specimens obtained from different anatomic sites. All specimens analyzed were diagnosed previously using morphologic and immunophenotypic methods, with molecular analysis in a subset of cases. The study group included 25 cases of MCL, including six lymph node (LN) biopsy specimens, five endoscopic biopsy specimens of the gastrointestinal tract (GI), two splenectomy (S) specimens, seven bone marrow (BM) aspirates, and five peripheral blood (PB) specimens. All cases of MCL were of classical small cell type and were immunohistochemically positive for cyclin D1 with variable intensity of staining. Four of 13 (31%) cases assessed by PCR for the t(11;14) were positive using methods described elsewhere (9). The study group also included 30 cases of chronic lymphocytic leukemia/small lymphocytic lymphoma (CLL/SLL), 14 cases of follicular lymphoma (FL) of all grades, 3 cases of marginal zone B-cell lymphoma (MZL), 1 case of diffuse large B-cell lymphoma, and 35 reactive or nonneoplastic specimens. The anatomic sites of these specimens are summarized in Table 1.

Four cell lines were also analyzed, including one with the t(11;14)(q13;q32), one plasma cell my-

Table 1. Summary of Cyclin D1/GAPDH Ratios According to Anatomic Site and Type of B-Cell Non-Hodgkin's Lymphoma

Site	NHL Type	Number	Cyclin D1/GAPDH
Lymph node (n = 22)	Mantle cell lymphoma	6	147 (94–160)
	Chronic lymphocytic leukemia	6	8.6 (4–18)
	Follicular lymphoma	4	5.8 (1.8–24)
	Marginal zone lymphoma	1	4.8
	Reactive	5	20.2 (5.8–44)
GI tract (n = 9)	Mantle cell lymphoma	5	82.7 (31.4–236)
	Diffuse large B-cell lymphoma	1	20
	Reactive	3	24.2 (12.5–25)
Spleen (n = 5)	Mantle cell lymphoma	2	76.8 (64.2–89.3)
	CLL/SLL	1	15.2
	Reactive	2	23.9 (16.4–31.3)
Bone marrow (n = 54)	Mantle cell lymphoma	7	15.4 (4–110)
	CLL/SLL	19	0.42 (.07–2.0)
	Follicular lymphoma	5	0.04 (.03–.07)
	Marginal zone lymphoma	2	0.25 (.20–0.29)
	Non-neoplastic*	21	0.19 (.04–1.5)
Peripheral blood (n = 18)	Mantle cell lymphoma	5	34.5 (2.9–350)
	Follicular lymphoma	5	0.11 (.05–.28)
	CLL/SLL	4	0.68 (.14–1.1)
	Non-neoplastic**	4	0.10 (.01–0.25)
Total n = 108			

* This group includes patients without non-Hodgkin's lymphoma and patients with a history of non-Hodgkin's lymphoma (including mantle cell lymphoma) in complete clinical remission with no morphologic or immunophenotypic evidence of disease at the time these bone marrow aspirates were obtained.

** All 4 patients in this group had a history of mantle cell lymphoma. These patients were in complete clinical remission with no morphologic or immunophenotypic evidence of disease at the time these peripheral blood specimens were obtained.

eloma cell line, and two with the t(14;18)(q32;q21) involving the major (MBR) and minor (MCR) breakpoint cluster regions of the *bcl*-2 gene, respectively (all gifts from Richard Ford, M.D., Ph.D.). In each specimen, GAPDH mRNA levels were also quantified to normalize cyclin D1 mRNA levels and to serve as a control.

RNA was extracted from all specimens using the Trizol reagent (Invitrogen Life Technologies, Carlsbad, CA). Briefly, RNA was extracted from 2 to 50 mg of tissue or from 250 μL of PB or BM according to the manufacturer's instructions. Depending on the pellet size, the RNA recovered was suspended in 10–20 μL of RNase-free water and the samples were stored at −70° C until time of analysis. One microliter of diluted RNA was used for each reaction.

5' → 3' Exonuclease-Based Real-Time RT-PCR Method

Using a one-step RT-PCR, cyclin D1 and GAPDH mRNA were amplified in separate tubes using a 5' → 3' exonuclease-based real-time quantitative RT-PCR assay and the PRISM 7700 Sequence Detector (PE Applied Biosystems, Foster City, CA). This instrument is an integrated system consisting of a thermal cycler, a laser for fluorescence induction, and a charge-coupled device that detects fluorescence as a result of PCR amplification.

The principles of 5' → 3' exonuclease-based real-time PCR assays have been described by other investigators (20–22). Briefly, each probe is labeled with two fluorescent dyes, a 5' reporter dye and a 3' quencher dye. During the extension phase of PCR, the 5' → 3' exonuclease activity of *Taq* polymerase cleaves the reporter dye from the probe, resulting in increased fluorescence. The fluorescence signal is collected and monitored by the PRISM 7700 Sequence Detector. The online software system analyzes the spectral data collected during the extension phase of each cycle and plots fluorescence intensity *versus* cycle number. The fluorescence data is expressed as Rn or △Rn, where Rn (normalized reporter signal) is the fluorescence signal of the reporter dye divided by the fluorescence signal of the passive internal reference dye. △Rn is Rn minus the baseline signals established during the first few cycles of PCR.

The primers and probes used in this assay to amplify cyclin D1 and GAPDH mRNA are listed in Table 2. The forward and reverse primers for each target are derived from different exons to avoid contamination by genomic DNA and generate amplicon sizes of 75 bp for cyclin D1 (GenBank Accession No. M64349) and 226 bp for GAPDH (GenBank Accession No. J04038). For the cyclin D1 and GAPDH probes, we used 6-carboxy fluorescein (FAM) and 2',7'-dimethoxy-4',5'-dichloro-6-carboxyfluorescein (JOE), respectively, as the 5' reporter dye. N,N,N',N'-tetramethyl-6-carboxyrhodamine (TAMRA) was the 3' quencher dye for both probes. Cyclin D1 expression levels in test specimens were expressed as the ratio of cyclin D1 to GAPDH.

Fifty nanograms of total RNA isolated from the HL60 cell line were serially diluted in water to obtain dilutions of 50, 5, 1, 0.5, and 0.1 ng. This allowed generation of standard curves for both cyclin D1 (Fig. 1A–B) and GAPDH (Fig. 2A–B) expression.

Analytical Sensitivity of Assay

Assay sensitivity was assessed by quantifying cyclin D1 levels in serial dilutions of the t(11;14)-positive MCL cell line. In this experiment, 10^6 cells of the MCL cell line were serially diluted with cells from one of the t(14;18)-positive cell lines, resulting in 10^{-1} to 10^{-5} dilutions. The t(14;18)-positive cell line was used because its level of cyclin D1 expression is comparable to that of normal peripheral blood lymphocytes and thus can be used to approximate the sensitivity of this assay *in vivo*. The RNA extracted from each dilution was suspended in 10 μL of RNase-free water. One microliter of total RNA was then subjected to one-step real-time RT-PCR for cyclin D1 (Fig. 3A–B) and GAPDH in duplicate. As each dilution consisted of 10^6 cells, the GAPDH levels were essentially the same in all dilutions (data not shown).

Correlation with Tumor Burden

In all five PB specimens involved by MCL, flow cytometry immunophenotypic studies were per-

Table 2. Primers and Probes Used in Real-Time Quantitative Reverse Transcription Polymerase Chain Reaction Assay

Primer or Probe	Nucleotide Position
Cyclin D1	
Forward 5′ -CCGTCCATGCGGAAGATC-3	304
Reverse 5′ -GAAGACCTCCTCCTCGCACT-3	−378
Probe 5′ -FAM TCTGTTCCTCGCAGACCTCCAGCA-TAMRA-3	
GAPDH	
Forward 5′ -GAAGGTGAAGGTCGGAGT-3	1459
Reverse 5′ -GAAGATGGTGATGGGATTTC-3	−3388
Probe 5′ -JOE CAAGCTTCCCGTTCTCAGCC-TAMRA-3	

GAPDH, glyceraldehyde - 3 - phosphate dehydrogenase; FAM, 6-carboxyfluorescein (FAM); TAMRA, N,N,N′,N′-tetramethyl-6-carboxyrhodamine; JOE, 2′,7′-dimethoxy-4′,5′-dichloro-6-carboxyfluorescein.

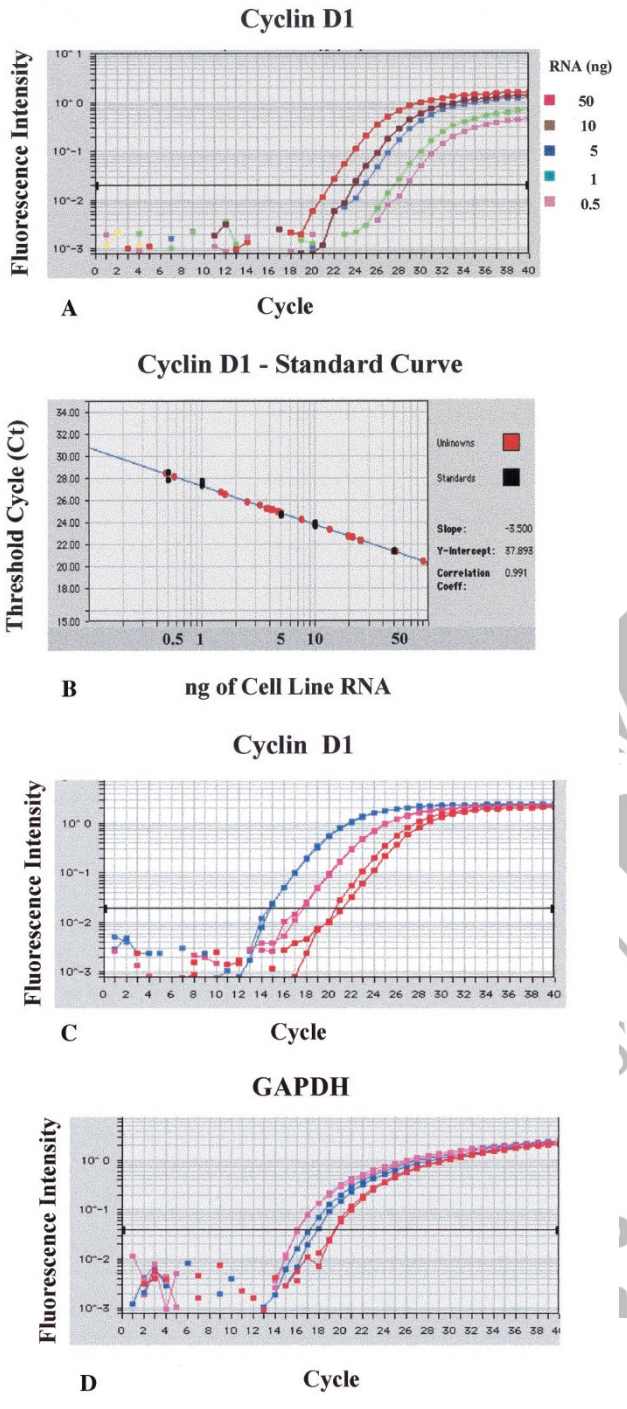

FIGURE 1. **A,** total RNA isolated from the HL60 cell line serially diluted to obtain dilutions ranging from 50 to 0.1 ng from which cyclin D1 was amplified by real-time reverse transcriptase-polymerase chain reaction (RT-PCR). Amplification is shown in logarithmic scale. **B,** threshold cycle plotted against nanograms of HL60 cell line RNA to obtain a standard curve. **C and D,** representative cases of mantle cell lymphoma (**blue**), chronic lymphocytic leukemia/small lymphocytic lymphoma (**pink**), and follicular lymphoma (**red**) amplified for cyclin D1 (**C**) and GAPDH (**D**) by RT-PCR (specimens analyzed in duplicate).

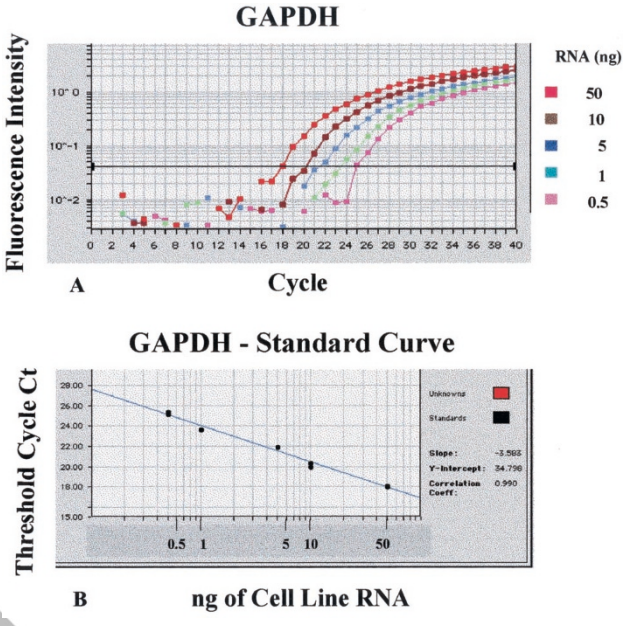

FIGURE 2. Total RNA isolated from serial dilutions of the HL60 cell line was analyzed for GAPDH as described in Methods. **A,** amplifications are shown in logarithmic scale (analyzed in duplicate). **B,** standard curve showing input RNA concentration *versus* threshold cycle.

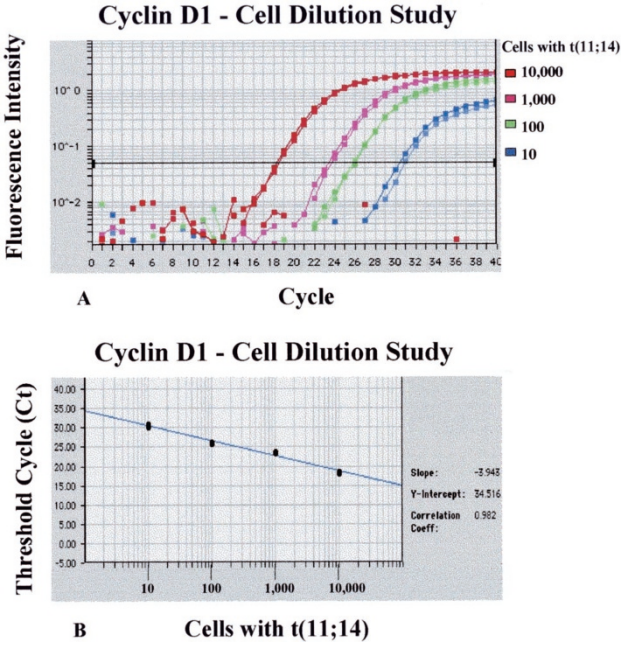

FIGURE 3. Dilution analysis illustrating the threshold sensitivity of this real time RT-PCR assay for detecting cells that overexpress cyclin D1. **A,** a mantle cell lymphoma cell line that carries the t(11;14) and overexpresses cyclin D1 was diluted into a t(14;18)-positive cell line that expresses a negligible level of cyclin D1, comparable to that of normal peripheral blood lymphocytes, and was analyzed using this real time RT-PCR assay to assess for cyclin D1 overexpression (specimens analyzed in duplicate). **B,** standard curve generated using the fluorescence data collected in exponential phase of the dilution study.

formed using a variable panel of antibodies that included antibodies specific for CD5 and CD19. We estimated tumor burden by multiplying the absolute lymphocyte count by the percentage of lymphocytes positive for both CD5 and CD19.

To estimate MCL tumor burden in BM, the percentage of lymphocytes in BM aspirate smears and the percentage of tumor cells that replaced clot or biopsy specimens were assessed.

Statistical Analysis

To establish the statistical significance of observed cyclin D1/GAPDH ratios among multiple groups, one-way analysis of variance (ANOVA) was used, followed by Tukey's pairwise comparison for normally distributed data points or Dunn's test for non-normally distributed data. For pairs of normally distributed groups, the two-tailed *t* test was used. Correlation between relative cyclin D1 levels and tumor burden was assessed by linear regression analysis and by calculating Pearson's correlation coefficient. We used Jandel's Sigmastat software (High Text Interactive, San Diego, CA).

RESULTS

Cyclin D1 and GAPDH mRNA were detected in all specimens tested (Fig. 1C–D and Table 1). The cyclin D1/GAPDH ratio ranged from 0.01 to 350. Cyclin D1 levels were highest in specimens involved by MCL, and there was no overlap with other types of B-cell NHL or with nonneoplastic specimens at each anatomic site (Table 1).

Tissue Specimens

In LN specimens involved by MCL, the median cyclin D1/GAPDH ratio was 147 (range, 94–160), which was higher than LN specimens involved by CLL/SLL (8.6; range, 4–18), FL (5.8; range, 1.8–24), 1 case of MZL (4.8), and reactive specimens (20.2; range, 5.8–44). There was no correlation between histologic pattern and cyclin D1GAPDH ratio in six LN specimens involved by MCL, although no cases with a pure (>90%) mantle zone pattern were analyzed.

Statistical analysis by ANOVA showed that relative cyclin D1 levels in MCL were significantly different from all other groups ($P < .05$) whereas no significant differences were found between the various non-MCL groups. Combining all non-MCL cases, a relative cyclin D1 level of 13.2 ± 11.5 was obtained for the non-MCL group, *versus* 137.5 ± 25.6 for the MCL group. Because the data were normally distributed, cutoff values could be established based on mean ± standard deviation (SD). The mean − 3 SD value for MCL cases was 60.7, which does not overlap with the mean +3 SD value for non-MCL cases, 47.7. Thus, by selecting these cutoffs,, a diagnostically useful separation can be achieved ($P < .01$).

In GI and S specimens involved by MCL, cyclin D1/GAPDH ratios were also higher than other types of NHL or reactive specimens. The median cyclin D1/GAPDH ratio was 82.7 (range, 31.4–236) in GI specimens and 76.8 (range, 64.2–89.3) in S specimens. Reactive specimens had slightly higher cyclin D1/GAPDH ratios than other types of B-cell NHL, with the highest ratio being 31.3. One case of diffuse large B-cell lymphoma and one case of CLL/SLL had cyclin D1/GAPDH ratios of 20.0 and 15.2, respectively. No statistically significant differences were found in either the GI or S specimens between the various groups, although there was a small number of GI and S specimens.

Combining all tissue (LN, GI, and S) specimens, there was no significant difference in levels of cyclin D1 expression between CLL/SLL and FL, but the sample numbers are small.

Peripheral Blood and Bone Marrow Specimens

Cyclin D1 levels were generally lower in BM and PB samples as compared with tissue specimens (Table 1). The median cyclin D1GAPDH ratios for BM and PB involved by MCL were 15.4 (range, 4–110) and 34.5 (range, 2.9–350), respectively. Similarly, in other types of B-cell NHL and in uninvolved specimens, the median cyclin D1GAPDH ratios were lower in BM and PB specimens as compared with tissue specimens.

As shown in Table 1, BM specimens in cases of MCL had a significantly higher cyclin D1/GAPDH ratio than FL ($P < .05$) and nonneoplastic ($P < .05$) specimens, but not CLL/SLL specimens (Kruskal-Wallis). Cyclin D1 levels were also significantly higher in CLL/SLL compared with in FL ($P < .05$) and in CLL/SLL compared with in nonneoplastic specimens ($P < .0005$). Although the median cyclin D1/GAPDH ratios of CLL/SLL and nonneoplastic specimens were only slightly different, 0.42 (range, 0.07–2.0) *versus* 0.19 (range, 0.04–1.5), the large number of cases in each group most likely explains the achievement of statistical significance. As the data are not normally distributed (as is true for PB specimens), a cutoff to distinguish MCL from other types of NHL could not be determined. After normalizing the distribution of the data by log transformation and employing a parametric test, cyclin D1/GAPDH ratios were significantly higher in MCL compared with in other groups ($P < .05$).

Peripheral blood specimens involved by MCL also had higher cyclin D1GAPDH ratios compared with CLL/SLL, FL, and nonneoplastic specimens. However, these differences were statistically significant only for MCL *versus* nonneoplastic specimens ($P < .05$) and MCL *versus* FL ($P < .05$).

As shown in Tables 3 and 4, there was a correlation between extent of involvement by MCL in PB specimens and the cyclin D1/GAPDH ratio. Four PB specimens were obtained from patients with MCL in complete clinical remission, with no morphologic or immunophenotypic evidence of tumor (Table 1). In these patients, the median cyclin D1/GAPDH ratio was 0.1 (range, 0.01 to 0.25). In contrast, in five PB specimens involved by MCL

Table 3. Mantle Cell Lymphoma Involving Peripheral Blood—Correlation Between Cyclin D1/GAPDH Ratio and Tumor Burden

Patient Number	Cyclin D1/GAPDH	Absolute CD5+CD19+ Count ($\times 10^9$/L)*
1	2.94	0.03
2	9.8	0.39
3	34.5	0.33
4	57.3	0.84
5	350	1.56

* Calculated by multiplying absolute lymphocyte count by percentage of CD5 and CD19 positive cells determined by flow cytometry immunophenotypic analysis.

Table 4. Mantle Cell Lymphoma Involving Bone Marrow—Correlation Between Cyclin D1/GAPDH Ratio and Tumor Burden

Patient Number	Cyclin DI/GAPDH	Bone Marrow	
		Aspirate Smear Lymphocytes* (%)	Tumor in Clot or Biopsy Section (%)
1	4	10	20
3	4.8	21	<5
3	8.6	21	5
4	15.4	6	10
5	22	18	5
6	70	6	60
7	110	63	40

* All lymphocytes (non-neoplastic and neoplastic).

(Table 3), cyclin D1 levels were generally higher in patients with a higher absolute number of CD5+ CD19+ (presumably tumor) cells. The number of circulating MCL cells showed a strong linear correlation with the relative cyclin D1 level ($r = 0.93$, $P = .02$). However, there were also exceptions in PB specimens in which the cyclin D1/GAPDH ratio was higher or lower than that expected for the estimate of tumor burden. For example, Case 3 had a slightly lower absolute CD5+ CD19+ count than that of Case 2 but had a cyclin D1/GAPDH ratio that was more than three times higher than that of Case 2.

A similar correlation in BM specimens between extent of involvement by MCL and cyclin D1 levels could not be established (using the logarithms of the variables, $r = 0.23$, $P = .62$ for aspirate smears; $r = 0.66$, $P = .11$ for clot biopsy sections). This lack of correlation indicates presumably that extrapolation of the percentage of lymphocytes in aspirate smears to tumor burden by this approach is inaccurate. Similarly, visual assessment of tumor percentage in histologic sections also appears to be an inaccurate estimate of tumor burden.

We also correlated the cyclin D1/GAPDH ratio with tumor burden in four cases of CLL/SLL involving PB. As flow cytometry immunophenotypic studies were not available for these cases, we used the absolute lymphocyte count determined by multiplying the percentage of lymphocytes determined by manual differential count by the total leukocyte count. There was no correlation between cyclin D1 level and absolute lymphocyte count.

Patients with Multiple Specimens

Seven patients had more than one specimen analyzed for cyclin D1 mRNA: four with MCL and three with CLL/SLL (Table 5). One patient with MCL had four specimens: LN, GI, PB, and BM. Three other MCL patients had both PB and BM assessed. In all MCL patients, PB had the higher and BM the lower cyclin D1/GAPDH ratios. Two

Table 5. Summary of Cyclin D1/GAPDH Ratios in Seven Patients with Multiple Specimens Analyzed

Patient Number	Diagnosis	PB	BM	LN	GI	S
1	MCL	350	110	120	100	—
2	MCL	9.8	4.8	—	—	—
3	MCL	34.5	8.6	—	—	—
4	MCL	57.3	15.4	—	—	—
1	CLL/SLL	0.41	0.95	—	—	—
2	CLL/SLL	0.14	0.42	—	—	—
3	CLL/SLL	—	0.35	—	—	15.2

PB, peripheral blood; BM, bone marrow aspirate; LN, lymph node; GI, gastrointestinal tract; S, spleen MCL, mantle cell lymphoma; CLL/SLL, chronic lymphocytic leukemia/small lymphocytic lymphoma.

patients with CLL/SLL had PB and BM specimens with no difference in cyclin D1 levels between these sites. One patient with CLL/SLL had a much higher cyclin D1 level in S than in BM.

Cell Line Analysis

The MCL cell line had a cyclin D1GAPDH ratio of 94.9. The plasma cell myeloma cell line had a cyclin D1/GAPDH ratio of 0.2. Both cell lines with the t(14;18)(q32;q21) had negligible levels of cyclin D1, with cyclin D1/GAPDH ratios of <0.05.

Analytical Sensitivity

In all dilutions (10^{-1} to 10^{-5}) of the MCL cell line into the t(14;18)-positive cell line, increased fluorescence signal could be detected. However, at the 10^{-5} dilution the fluorescence signal overlapped with background signal, suggesting that cyclin D1 overexpression can be detected reliably only when the MCL cell line constitutes $\geq 0.01\%$ of the total cells. In other words, this assay can detect 100 MCL cells in 10^6 total cells. This t(14;18)-positive cell line expresses a level of cyclin D1 comparable to normal peripheral blood lymphocytes.

DISCUSSION

Mantle cell lymphoma can be difficult to distinguish from other types of low-grade B-cell NHL. Thus, ancillary techniques to detect the t(11;14)(q13;q32) or cyclin D1 overexpression are valuable to support the diagnosis of MCL. In cases of MCL in which fresh or frozen tissue is not available, detection of cyclin D1 overexpression assumes greater importance.

In most pathology laboratories, immunohistochemical methods to detect cyclin D1 overexpression are popular for distinguishing MCL from other B-cell NHL. However, there are problems with this approach. First, cyclin D1 immunostaining can be technically challenging, even with the use of heat-induced epitope retrieval methods. Even optimal results do not compare with those obtained with other antibodies, such as L26 (CD20) and LCA (CD45). Bartkova and colleagues (19) have shown that delays before placing tissue in fixative substantially affect immunostaining intensity, which, at least in part, may explain suboptimal results. Second, immunohistochemical methods to assess cyclin D1 are optimized for formalin-fixed tissue. In our experience, cyclin D1 immunostaining is often unsuccessful using tissue fixed in B5, Zenkers, or other alternatives to formalin fixation. Lastly, we have had inconsistent results when we have performed immunohistochemical studies for cyclin D1 on PB and BM smears. Thus, a rapid method to assess for cyclin D1 overexpression in fluid specimens has potential value.

The results presented here demonstrate that this 5' → 3' exonuclease-based real-time RT-PCR method can be used to quantify cyclin D1 expression levels in B-cell NHL and nonneoplastic specimens. All types of B-cell NHL and benign specimens expressed at least minimal levels of cyclin D1. However, cases of MCL had substantially higher levels of cyclin D1, with median levels ranging from 4 to >30 times higher than that of other types of B-cell NHL, depending on the anatomic site. Furthermore, there was no overlap between the highest cyclin D1/GAPDH ratio in non-MCL NHL cases and the lowest cyclin D1/GAPDH ratio in MCL specimens at each anatomic site. Thus, this method appears to be a useful aid in the differential diagnosis of MCL with other low-grade B-cell NHL cases.

In this study, levels of cyclin D1 expression varied according to specimen type, which has implications for the establishment of normal reference ranges. In tissue specimens, reactive cases had generally higher cyclin D1 levels than cases of low-grade B-cell NHL, although much lower than those in MCL cases. For example, in LN specimens (Table 1), the median cyclin D1/GAPDH ratio for reactive specimens was 20.2, compared with 8.6 for CLL/SLL, 5.8 for FL, and 4.8 for MZL (only 1 case). We believe that the cyclin D1 levels in reactive LN and S specimens can be attributed to the vascularity within these specimens, as endothelial cells are known to express abundant cyclin D1 (6). We also histologically examined routinely processed tissue sections of the LN and S specimens analyzed in this study and confirmed that the reactive specimens had greater vasculature than the specimens involved by low-grade B-cell NHL. Reactive GI biopsy specimens also had appreciable cyclin D1 levels (median cyclin D1/GAPDH ratio 24.2), similar to that of reactive LN specimens. The most likely explanation for the cyclin D1 levels detected in the GI specimens is the presence of epithelial cells (as well as endothelial cells) that are known to express cyclin D1 (19, 23), as glandular cells were plentiful in the routinely processed histologic sections of these specimens. In contrast, uninvolved PB and BM specimens have extremely low levels of cyclin D1 expression, presumably related to the relatively low degree of vascularity and absence of epithelial cells in these specimens. Thus, normal reference ranges for cyclin D1 expression can be set much lower in PB and BM than in tissue specimens.

Previous studies using Northern blot analysis, immunohistochemical methods, and semiquantitative RT-PCR methods have suggested that nonneoplastic lymphoid tissues are negative for cyclin D1 (4, 18, 23, 24). However, it is clear from the data presented in this study that cyclin D1 mRNA is

expressed at low levels in reactive lymphoid tissues when assessed using the real-time RT-PCR methods, as also has been described by others (25). Although it is likely that most of the cyclin D1 expression can be attributed to the presence of endothelial or epithelial cells in reactive tissues, even in uninvolved PB and BM specimens, extremely low levels of cyclin D1 were detected in this study, suggesting that normal hematopoietic cells express low-levels of cyclin D1.

As shown in Table 3, in PB specimens there was a strong correlation between the cyclin D1GAPDH ratio and the extent of involvement by MCL. Using the PB absolute lymphocyte count and the percentage of CD5+ CD19+ cells (determined by flow cytometry immunophenotypic methods), the total number of MCL cells was approximated, and the cyclin D1/GAPDH ratio correlated significantly with the absolute count of CD5+ CD19+ cells ($r = 0.93$, $P = .02$). However, it appears that cyclin D1 expression levels may not only reflect tumor burden. For example, Case 3 in Table 3 had a lower number of CD5+ CD19+ cells than Case 2 but had a substantially higher cyclin D1/GAPDH ratio. These findings suggest that cases of MCL vary in the amount of cyclin D1 they express. This may explain, at least in part, the variation in immunostaining intensity observed in different cases of MCL analyzed immunohistochemically using routine methods.

Others have used RT-PCR methods to assess for cyclin D1 in MCL with results in general agreement with our own (18, 23, 25–28). In some of these studies, the presence or absence of cyclin D1 was considered the endpoint without quantification (23). In other studies, traditional semiquantitative methods RT-PCR methods have been employed (18, 26–28). Unlike these approaches, the 5' → 3' exonuclease-based quantitative real-time RT-PCR assay we describe is rapid, simpler and does not require an internal competitor or cumbersome dilution steps needed in traditional semiquantitative assays. Furthermore, real-time RT-PCR methods, such as the method we describe, collect data points in the exponential phase of PCR, unlike traditional semi-quantitative PCR methods that use endpoints, and thus quantification of target is more accurate. Two other research groups have used real-time RT-PCR approaches to quantify cyclin D1 expression similar to our own for these reasons (25, 29). In addition to the description of this method, our study further contributes to the literature by highlighting the need to account for anatomic site when establishing normal reference ranges and cutoffs for cyclin D1 expression. Our data also show a correlation between extent of involvement by MCL (i.e., tumor burden) and levels of cyclin D1 expression.

In four MCL patients with multiple specimens in this study, PB specimens had the highest cyclin D1 expression levels in each patient (Table 5). As described above, in patients with MCL involving PB, cyclin D1 levels correlated with extent of involvement (Table 3). In contrast, patients with MCL in complete remission had extremely low levels of cyclin D1 (Table 1). These data suggest that PB specimens may be useful for monitoring disease progression, response to therapy, and/or detection of minimal residual disease.

REFERENCES

1. Armitage JO, Weisenburger DD. New approach to classifying non-Hodgkin's lymphomas: clinical features of the major histologic subtypes. J Clin Oncol 1998;16:2780–95.
2. Motokura T, Arnold A. PRAD1/cyclin D1 proto-oncogene: genomic organization, 5' DNA sequence, and sequence of a tumor-specific rearrangement breakpoint. Genes Chromosom Cancer 1993;7:89–95.
3. Withers DA, Harvey RC, Faust JB, Melnyk O, Carey K, Meeker TC. Characterization of a candidate bcl-1 gene. Mol Cel Biol 1991;11:4846–53.
4. Zukerberg LR, Yang WI, Arnold A, Harris NL. Cyclin D1 expression in non-Hodgkin's lymphomas. Detection by immunohistochemistry. Am J Clin Pathol 1995;103:756–60.
5. deBoer CJ, Schuuring E, Dreef E, Peters G, Bartek J, Kluin PM, *et al.* Cyclin D1 protein analysis in the diagnosis of mantle cell lymphoma. Blood 1995;86:2715–23.
6. Lai R, Medeiros LJ. Pathologic diagnosis of mantle cell lymphoma. Clin Lymphoma 2000;1:197–206.
7. Medeiros LJ, Van Krieken JH, Jaffe ES, Raffeld M. Association of bcl-1 rearrangements with lymphoma of intermediate differentiation. Blood 1990;76:2086–90.
8. Williams ME, Swerdlow SH, Rosenberg CL, Arnold A. Characterization of chromosome 11 translocation breakpoints at the bcl-1 and PRAD1 loci in centrocytic lymphoma. Cancer Res 1992;52:5541s–4s.
9. Luthra R, Hai S, Pugh WC. Polymerase chain reaction detection of the t(11;14) translocation involving the bcl-1 major translocation cluster in mantle cell lymphoma. Diagn Mol Pathol 1995;4:4–7.
10. Pinyol M, Campo E, Nadal A, Terol MJ, Jares P, Nayach I, *et al.* Detection of the bcl-1 rearrangement at the major translocation cluster in frozen and paraffin-embedded tissues of mantle cell lymphomas by polymerase chain reaction. Am J Clin Pathol 1996;105:532–7.
11. Rimokh R, Berger F, Delsol G, Digonnet I, Rouault JP, Tigaud JD, *et al.* Detection of the chromosomal translocation t(11;14) by polymerase chain reaction in mantle cell lymphomas. Blood 1994;83:1871–5.
12. Luthra R, Sarris AH, Hai S, Paladugu AV, Romaguera JE, Cabanillas FF, *et al.* Real-time 5' → 3' exonuclease-based PCR assay for detection of the t(11;14)(q13;q32). Am J Clin Pathol 1999;112:524–30.
13. Remstein ED, Kurtin PJ, Buno I, Bailey RJ, Proffitt J, Wyatt WA, *et al.* Diagnostic utility of fluorescence *in situ* hybridization in mantle-cell lymphoma. Br J Haematol 2000;110:856–62.
14. Katz RL, Caraway NP, Gu J, Jiang F, Pasco-Miller LA, Glassman AB, *et al.* Detection of chromosome 11q13 breakpoints by interphase fluorescence in situ hybridzation. A useful ancillary method for the diagnosis of mantle cell lymphoma. Am J Clin Pathol 2000;114:248–57.
15. Coignet LJ, Schuuring E, Kibbelaar RE, Raap TK, Kleiverda KK, Bertheas MF, *et al.* Detection of 11q13 rearrangements

in hematologic neoplasias by double-color fluorescence *in situ* hybridization. Blood 1996;87:1512–9.
16. de Boer CJ, van Krieken JH, Kluin-Nelemans HC, Kluin PM, Schuuring E. Cyclin D1 messenger RNA overexpression as a marker for mantle cell lymphoma. Oncogene 1995;10:1833–40.
17. Bosch F, Jares P, Campo E, Lopez-Guillermo A, Piris MA, Villamor N, *et al.* PRAD1/cyclin D1 gene overexpression in chronic lymphoproliferative disorders: a highly specific marker of mantle cell lymphoma. Blood 1994;84:2726–32.
18. Aguilera NSI, Bijwaard KE, Duncan B, Kraft AE, Chu WS, Abbondanzo SL, *et al.* Differential expression of cyclin D1 in mantle cell lymphoma and other non-Hodgkin's lymphomas. Am J Pathol 1998;153:1969–76.
19. Bartkova J, Lukas J, Strauss M, *et al.* Cell cycle-related variations and tissue-restricted expression of human cyclin D1 protein. J Pathol 1994;172:237–45.
20. Holland PM, Abramson RD, Watson R, Gelfand DH. Detection of specific polymerase chain reaction product by utilizing the 5' → 3' exonuclease activity of Thermus aquaticus DNA. Proc Natl Acad Sci U S A 1991;88:7276–80.
21. Heid CA, Stevens J, Livak KJ, Williams PM. Real-time quantitative PCR. Genome Res 1996;6:986–94.
22. Luthra R, Medeiros LJ. 5' → 3' exonuclease-based real-time PCR methods for detecting the t(14;18) and t(11;14) in non-Hodgkin's lymphomas. J Clin Ligand Assay 2000;23:6–14.
23. Athanasiou E, Kotoula V, Hytiroglou P, Kouidou S, Kaloutsi V, Papadimitriou CS. In situ hybridization and reverse transcription-polymerase chain reaction for cyclin D1 mRNA in the diagnosis of mantle cell lymphoma in paraffin-embedded tissues. Mod Pathol 2001;14:62–71.
24. Oka K, Ohno T, Kita K, Yamaguchi M, Takakura N, Nishii K, *et al.* PRAD1 gene over-expression in mantle-cell lymphoma but not in other low-grade lymphomas, including extranodal lymphoma. Br J Haematol 1994;86:786–91.
25. Bijwaard KE, Aguilera NS, Monczak Y, Trudel M, Taubenberger JK, Lichy JH. Quantitative real-time reverse transcription-PCR assay for cyclin D1 expression: utility in the diagnosis of mantle cell lymphoma. Clin Chem 2001;47:195–201.
26. Uchimaru K, Taniguchi T, Yoshikawa M, Asano S, Arnold A, Fujita T, *et al.* Detection of cyclin D1 (bcl-1, PRAD1-) overexpression by a simple competitive reverse transcription-polymerase chain reaction assay in t(11;14)(q13;q32) bearing B-cell malignancies and/or mantle cell lymphoma. Blood 1997;89:965–74.
27. Sola B, Salaun V, Ballet JJ, Troussard X. Transcriptional and post-transcriptional mechanisms induce cyclin-D1 overexpression in B-cell chronic lymphoproliferative disorders. Int J Cancer 1999;83:230–4.
28. Sola B, Roue G, Duquesne F, Avert-Loiseau H, Macro M, Salaun V, *et al.* Expression of cyclins D-type in B-chronic lymphoproliferative disorders. Leukemia 2000;14:1318–9.
29. Suzuki R, Takemura K, Tsutsumi M, Nakamura S, Hamajima N, Seto M. Detection of cyclin D1 overexpression by real-time reverse-transcriptase-mediated quantitative polymerase chain reaction for the diagnosis of mantle cell lymphoma. Am J Pathol 2001;159:425–9.

Book Review

McCarthy DA and Macey MC, editors: Cytometric Analysis of Cell Phenotype and Function, 430 pp, Cambridge, Cambridge University Press, 2001 ($140.00).

Flow cytometry is a rapidly developing technique. No matter how the books on flow cytometry are prepared, they are destined to be outdated in a few years. This textbook is written by multiple authors from each expertise and consists of 18 chapters. The chapters on principles of flow cytometry are basically the same as in other books on the same subject. Practical usage of flow cytometry is the major interest for practicing pathologists, whose interests go beyond hematopathology. The following five topics are most useful for practicing pathologists: 1) Immunophenotyping of leukemia and lymphoma, 2) CD 34 counting for autotransplants, 3) CD 4/CD 8 ratio in HIV-infected patients, and 5) DNA analysis of solid tumors.

The immunophenotype of hematological malignancies and leukocytes in disease are probably the most useful chapters to the practicing pathologists. Each chapter has concise basic principles of cytometric data, which are accompanied by light microscopic pictures of the cells relocated in the flow cytometric illustration. Each chapter also contains the protocols explaining adequate samples, methods, and analysis, which are extremely useful to the pathologist with an intention to pursue more investigation.

Cell cycle, DNA, and DNA ploidy analysis are widely used as research tools whether the information derived is useful or not in the practice of medicine. Cyclin dependent kinases and their inhibitors will be widely used for human tumors as analysis of human tumors is focused on cell cycle analysis as many antibodies are currently available for that investigation.

There is a limitation in resources in how many CD antibodies are used for the diagnosis of lymphoproliferative disorder. Despite the fact that about 250 CDs are listed, the total of CDs used in the community hospitals is relatively limited. Perhaps a minimal requirement for immunophenotyping of lymphoproliferative disorders, followed by more immunophenotyping and investigative phenotyping, may be subsequently listed as a guideline for nonhematology pathologists.

This book is well written, well edited, precise, and concise, as is usually the case with British authors.

Tatsuo Tomita
University of Kansas School of Medicine
Kansas City, Kansas